Physicochem. Probl. Miner. Process., 58(3), 2022, 147790

http://www.journalssystem.com/ppmp

Physicochemical Problems of Mineral Processing

ISSN 1643-1049

Study of flocculation performance and mechanism of ultrafine montmorillonite particles with NPAM

Lujun Wang, Fanfei Min, Jun Chen, Ting Wang, Zhuang Zhou

Department of Materials Science and Engineering, Anhui University of Science and Technology, Huainan 232001, China

Corresponding author: ffmin@aust.edu.cn (Fanfei Min)

Abstract: Ultrafine montmorillonite particles are the main clay minerals in industrial wastewater. In order to explore the flocculation performance and mechanism of flocculant with montmorillonite, the effects of nonionic polyacrylamide (NPAM) dosage and molecular weight on flocculation effect were studied using a flocculation sedimentation experiment. The morphology of flocs was observed by metallographic microscope and scanning electron microscope, and the microscopic adsorption mechanism was studied utilizing density functional theory (DFT). The results show that the best reagent system for the montmorillonite sample is that the molecular weight of NPAM is 14 million and the added amount is 100 g/t. The floc size increases with rising NPAM dosage, forming a unique multi-level compact space network structure through polymer bridging. The adsorption energy of acrylamide on the Na-(001) surface of montmorillonite is -108.81 kJ/mol, which is significantly higher than -50.66 kJ/mol on the None-(001) surface. Hydrogen bonding is not the main reason for the adsorption of acrylamide on the montmorillonite surface. NPAM mainly causes the flocculation and sedimentation of montmorillonite through the processes of polymer bridging and electrostatic attraction. This study can provide a theoretical basis for the design and synthesis of new flocculants.

Keywords: montmorillonite, flocculant, nonionic polyacrylamide, density functional theory

1. Introduction

The widespread application of the wet coal preparation process had resulted in the creation of large amounts of slime water. The quality of slime water treatment is the key to economic and environmental benefits, and is also one of the key links in the coal preparation plant production (Yu et al., 2017; Zhao et al., 2020). Although the properties of slime water in different coal preparation plants do vary, it is generally composed of clay minerals, oxide minerals, sulfide minerals, sulfate minerals, carbonate minerals and a large number of coal particles. Among them, clay minerals (mainly kaolinite, montmorillonite, illite) and quartz, which account for more than 60% of the total mineral mass, are the main reasons for the difficulties encountered in coal slurry treatment (Lin et al., 2010; Yan et al., 2021). On the one hand, these clay minerals have special crystal structures, which are prone to argillization and impact cracking, and thus produce a large number of hard-to-treat slurry. Meanwhile, these mineral particles have selective adsorption, dissolution, hydration and lattice substitution in water, which negatively charges the particles, and form an electrical double layer and hydration film. The result is electrostatic repulsion and steric hindrance effect (Feng et al., 2013; Kim et al., 2020). It not only affects the flotation (Bai et al., 2020) but also aggravates the difficulty of coal slime water sedimentation and dehydration (Doi et al., 2019).

The coal slime water system is complex and diverse, and the treatment methods and effects are different (Gong et al., 2016; Doi et al., 2019; Wang et al., 2019; Wang et al., 2020). At present in the coal preparation plant slime water treatment, polymer flocculant nonionic-polyacrylamide (NPAM) flocculation settlement is the most commonly employed. However, due to the different properties of mineral processing wastewater produced by various coal preparation plants and the different contents of various minerals, the treatment effects of NPAM on them are wide-ranging. Therefore, in order to better solve the problem of flocculation settlement of slime water, it is necessary to understand its nature

DOI: 10.37190/ppmp/147452

and composition, especially the behavior and mechanism of flocculation settlement of minerals with high content. Many studies have been published on the flocculation settlement laws of suspended particles in slime water (Chen et al., 2015, 2019; Y. Li et al., 2019; Kim et al., 2020; Yan et al., 2021; Zhu et al., 2021). Montmorillonite not only has large surface activity, but can also change the fluid characteristics of the liquid. The repulsion between the layers of -Si-O tetrahedron and -Al-O octahedron units in its structure enables the interlayer to have strong water absorption, so montmorillonite is one the most significant minerals in the clay mineral particles causing the refractory settlement of slime water (Peng et al., 2016; Yang et al., 2018; Ma et al., 2018). Yan et al. (Yan and Zhang, 2014) studied the adsorption and desorption mechanism of polyacrylamide (PAM) on pure kaolinite and montmorillonite by standard series of flocculation tests and isothermal adsorption method. The results showed that the adsorption capacity of the two clay minerals on three different types of PAM was in the order of non-ionic > cationic > anionic. The flocculation capacity of both clays is cationic > non-ionic > anionic. Deng et al. (Deng et al., 2006) studied the bonding mode between PAM and montmorillonite by Fourier transform infrared spectroscopy and X-ray diffraction analysis. Mpofu et al. (Mpofu et al., 2004) studied the effects of PAM and non-ionic polyethylene oxide (PEO) structure types on the flocculation, interface chemistry, particle interaction and dehydration behavior of montmorillonite dispersion by means of electric potential measurement, rheology measurement and scanning electron microscopy. There are other studies that are similar (Akimkhan, 2013; Fijałkowska et al., 2019; McFarlane et al., 2008; Vanerek et al., 2006; Wiśniewska et al., 2019, 2018). Although a number of experiments have investigated the mechanism of interaction between polyacrylamide and montmorillonite surfaces, it would be much clearer if the interaction between polymers and solid surfaces could be visualized at the molecular level. By constructing a reasonable molecular system, a molecular simulation method can study the law of molecular motion and interaction in the system, and obtain the desired outcomes that cannot be observed by macroscopic experiments (Lou et al., 2014; Han et al., 2016; Forrer et al., 2019). The process of interaction between reagents and minerals is studied from the microscopic point of view, and the mechanism of action between reagents and mineral surface is revealed. The results of Sun et al. (Sun et al., 2021) showed that the adsorption of inhibitor NW-1$^+$ on the surface and inner surface of Na-(001) was mainly due to electrostatic interaction. The adsorption on None-(001) surface was the result of the synergistic effect of electrostatic attraction and hydrogen bond. Li et al. (Li et al., 2021)studied the adsorption behavior of heavy metal ions on the surface of charged montmorillonite and concluded that polarization-induced covalent bond is a strong adsorption force. Peng et al. (Peng et al., 2016) also discovered that water molecules are mainly electrostatically adsorbed on the (001) surface of montmorillonite and hydrogen bond adsorption occurs on the (010) surface. Polymer flocculants are commonly used in industrial wastewater treatment, and montmorillonite especially so. Only a few studies have been done on the microscopic adsorption mechanism of polymer flocculants on the surface of montmorillonite.

Therefore, in this paper, experimental combined with simulation research ideas, montmorillonite was the subject of this research, using different molecular weight and dosage of NPAM for flocculation settlement experiment. The objective was to find the law of flocculation settlement. The floc state was observed by metallographic microscope and scanning electron microscope (SEM), while the flocculation effect and mechanism were analyzed intuitively. Meanwhile, based on the density functional theory, the adsorption behavior of acrylamide (AM) on the surface of montmorillonite was calculated and simulated. Through the calculation of adsorption energy, density of states analysis and electron density difference analysis, the microscopic adsorption mechanism of AM on the surface of montmorillonite was explored. This study aims to provide some theoretical basis for the treatment of slime water and the design of new and efficient flocculants.

2. Materials and methods

2.1. Materials

The montmorillonite samples were purchased from Zhejiang Fenghong Co., Ltd. Approximately 0.60 g dried sample was pressed into 2 mm thin slices by FW-4A tablet machine at 30 MPa. The contact angle was measured by SL200B dynamic / static contact angle meter, and the contact angle between montmorillonite and water was θ=30.9°, indicating that the montmorillonite sample had good

wettability. The mineral composition of montmorillonite samples was analyzed with a Rigaku X-ray diffractometer. The X-ray diffraction test conditions were: powder X-ray diffraction (XRD, Ultima IV, Rigaku) with Cu-Ka radiation was used to characterize the phase composition and crystal structures of all samples. The XRD data were obtained between 2θ values of 2° to 80° at a scanning speed of 5° with a count time of 2 s. The original data were incorporated into a diffraction diagram using Origin 8.0 software, and the results were calibrated by phase retrieval analysis of the montmorillonite sample. Results are shown in Fig. 1 (a).

From Fig. 1 (a), montmorillonite samples are mainly composed of montmorillonite and contain a small amount of quartz and other minerals. Meanwhile, the composition of montmorillonite sample is shown in Table 1. Compared with the ratio of elements in the molecular formula of montmorillonite, the purity of montmorillonite particles used in the experiment is very high, which can meet the requirements of this experiment.

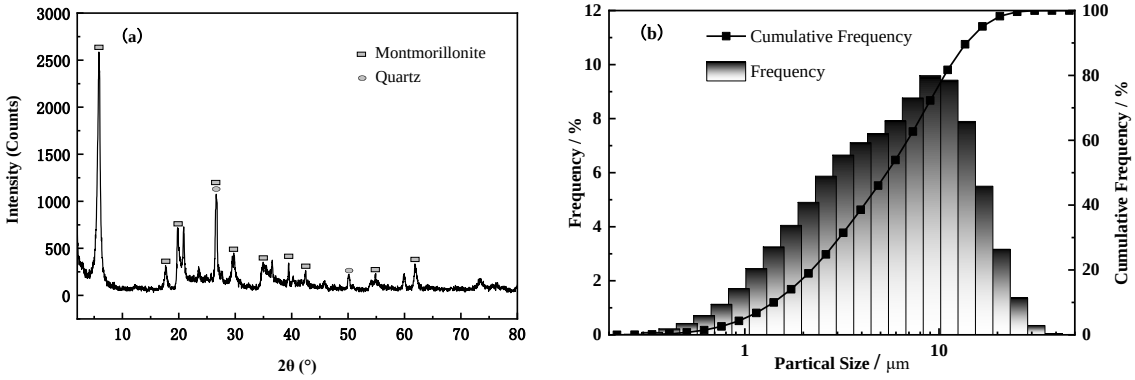

Fig. 1. Properties of montmorillonite samples

Table 1. Chemical composition of montmorillonite samples

Compound	SiO_2	Al_2O_3	Na_2O	MgO	CaO	Fe_2O_3
Wt%	67.44	17.91	3.96	2.40	3.21	2.83

In this paper, the particle size composition of montmorillonite is analyzed by the Japanese Shimadzu SALD-7101 laser particle size analyzer, and results are shown in Fig. 1 (b). They reveal that the particle used for the experiment size of montmorillonite is less than 45μm whose size is concentrated in 3~13μm. It belongs to the category of fine mineral particles and therefore can meet the research needs.

The experiment reagent is non-ionic polyacrylamide (NPAM) with molecular weights of 5 million, 7 million, 10 million, 14 million, 16 million and 18 million, respectively. The above NPAMs are analytically pure, the density is 1.189 g/mL at 25 °C, and purchased from Shanghai Macklin Biochemical Technology Co., Ltd. The NPAM structure is shown in Fig. 2.

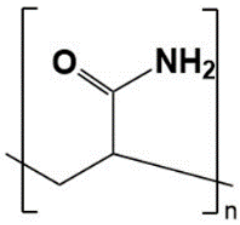

Fig. 2. The structural formula of nonionic polyacrylamide (NPAM)

2.2. Experimental methods

2.2.1. Flocculation sedimentation experiments

The specific flocculation sedimentation experiment proceeded as follows. First the montmorillonite suspension was established with pulp concentration of 20g/L, and subjected to a constant temperature

magnetic stirring for 10 min. Then it was mixed evenly and transferred to a measuring device with a scale, and a pipette served to absorb the corresponding amount of flocculant into the measuring device. The amounts of flocculant used in this experiment were 25g/t, 50g/t, 75g/t, 100g/t,125g/t and 150g/t, respectively. Flocculants were prepared according to the GB/T 18712-2002, and the mass concentration was 0.05%. Immediately after this an electrical stirrer was set to a specific speed for a stipulated period of time, `and the descending height of the clarification interface after timing was recorded. After settling for 10 minutes, the height of the bottom compression body, and measure turbidity removal rate and sedimentation yield were recorded. The experimental water comprised deionized water.

2.2.2. Initial settlement velocity experiments

In the flocculation sedimentation experiment, the descending height of the clarification liquid level was recorded when the time is started. The settlement velocity curve of the clarification interface was drawn, and the initial settlement velocity was calculated according to the formula (1) depicted below (according to the MT 190-88):

$$v = \frac{M\sum_{i=A}^{B} TiHi - (\sum_{i=A}^{B} Ti)(\sum_{i=A}^{B} Hi)}{M\sum_{i=A}^{B} T_i^2 - \sum_{i=A}^{B} T_i} \quad (1)$$

where: v is the initial settling velocity of the clarified interface (mm/s), Ti means a cumulative moment (i=0、1、2、3……n) (s), Hi represents the cumulative drop distance of the clarified interface corresponding to Ti (mm), A and B respectively denote the sequence number of the starting and ending type value points of the line segment (General A=1), and M is the cumulative number of type points from A to B.

2.2.3. Turbidity removal rate experiments

Ten minutes into the flocculation sedimentation experiment the time was stopped, and the supernatant at 10 ml below the liquid level was placed in a turbidity meter with a siphon. The data were read three times to calculate the average value, which is the turbidity of the supernatant of the experiment, and then the turbidity removal rate was calculated according to formula (2) (Guo et al., 2019):

$$R = \frac{T_0 - T_t}{T_0} \times 100\% \quad (2)$$

where R represents turbidity removal rate, T_0 stands for turbidity of the supernatant of original sample (NTU), and T_t is turbidity of supernatant after flocculation (NTU).

2.2.4. Sedimentation yield experiments

The bottom 100 ml suspension in the graduated cylinder was transferred to a 250ml beaker, put into a vacuum drying oven so it could completely dry. This was followed by weighing and recording the data, and calculating the sedimentation yield according to formula (3) (according to the MT 190-88):

$$W = \frac{M_t}{M_0} \times 100\% \quad (3)$$

where: W is the sedimentation yield, M_0 denotes the mineral weight after flocculation (g), and M_t stands for the initial mineral weight (g).

2.2.5. Zeta potential test

The Zeta potential measurement is carried out in Zetasizer Nano ZS 90 potential analyzer. When measuring, take out the U-shaped tube first, clean the U-shaped tube with ultrapure water, and then rinse the U-shaped tube with the solution to be tested. Finally, fill the U-shaped tube with the solution to be tested and put it into the instrument for automatic testing.

2.2.6. Size analysis of flocs

Different amounts of NPAM were added to montmorillonite suspension with a concentration of 20g/L. After the settlement of montmorillonite suspension and the clarification of supernatant, the

bottom floc was sucked out with a long rubber head dropper and dropped onto the glass slide. The glass slide was moved to the DMM-900C metallographic microscope for floc size observation.

2.2.7. Micromorphology analysis of flocs

After the montmorillonite suspension was settled, the bottom flocculating compression body was taken and placed on the slide. After natural air drying, the micromorphology of the floc was observed by using Flex scanning electron microscope to analyze its flocculation mechanism.

2.3. Computational models and methods

In this paper, the montmorillonite model consistent with Voora (Voora et al., 2011) was used for analysis, in which Al was replaced by Mg in the pyrophyllite model, and Na cation was added between the layers. In the model used, one Al in each cell was replaced by Mg, and the replacement structure was $Na_2[(MgAl_3O_8(OH)_4(Si_8O_{12})]_2$. The subsequent cell optimization and surface adsorption were studied based on this model. The crystal type of montmorillonite is of the TOT variety, there is a balanced cation Na ion between the unit layers, and the two surfaces are connected by Van Der Waals force. When the montmorillonite is cleaved along the (001) crystal plane, Na ions may enter the upper or lower planes. Subsequently, two types of surfaces are assumed to form: one is the surface with Na ions, denoting Na-(001) surface; and the other is without, denoting None-(001) surface (Shi et al., 2013 , 2014). The single crystal along the (001) plane was cut, using a 2×1×1 supercell model, and a vacuum layer of 20Å added on the surface model. Two kinds of surface layer crystal models of montmorillonite Na-(001) and None-(001) were constructed. While calculating the adsorption model, the bottom two atoms of the surface structure were fixed, while the other atomic layers on the surface relaxed.

The CASTEP module based on density functional theory in Materials Studio software was used for calculation purposes. The GGA-PBE function served as the exchange correlation function for the optimization of the montmorillonite phase lattice and surface structure model, and the plane wave truncation energy was set to 400eV(Ren et al., 2020). Ultrasoft-pseudopotential was used to describe the interaction between Valence Electrons and Ion Cores. BFGS algorithm helped to optimize the model and calculate its properties, and the self-consistent field convergence accuracy was set as 1.0×10-6eV/atom. Geometric optimization convergence criteria were as follows this article (Peng et al., 2016). According to the Monkhorst-Pack method, the k-point sampling in the Brillouin zone of montmorillonite phase was set as (2×2×1), and the surface model k-point was set as (restricted to) the Gamma point. The structure of the acrylamide monomer model was optimized in the lattice of 20Å×20Å×20Å, and k-point was set as the Gamma point. Electron density difference analysis helps to calculate the differential electron density of acrylamide monomer by Edit Sets defining AM DensityDifference. All the calculations were carried out in reciprocal space, and the valence electrons selected for the pseudopotential calculations involving atoms were Al $3s^23p^1$, Si $3s^23p^2$, O $2s^22p^4$ and H $1s^1$, respectively. During the calculation, all adsorption models were not charged by default.

3. Results and discussion

3.1. Experimental result analysis

3.1.1. Influence of molecular weight of NPAM on flocculation sedimentation

The flocculation and sedimentation effect of montmorillonite under the actions of different molecular weight NPAM was studied. For this part of the experiment the fixed dosage was 100 g/t, as shown in Fig. 3.

Before adding NPAM, a blank control experiment was carried out and this meant no agents were added to make it settle naturally. The results show that the sedimentation yield was 66.41% and the supernatant turbidity was 4472.0NTU. It can be seen from Fig. 3 (a) that adding the molecular weight of NPAM can effectively improve flocculation. With the increase in the molecular weight of NPAM, the law of the sedimentation yield and turbidity removal rate of the supernatant are basically the same: at first, they clearly increased to a certain optimal value, then began to decrease slightly. As for the experimental index of compression body height, it first increases and then decreases continuously. This

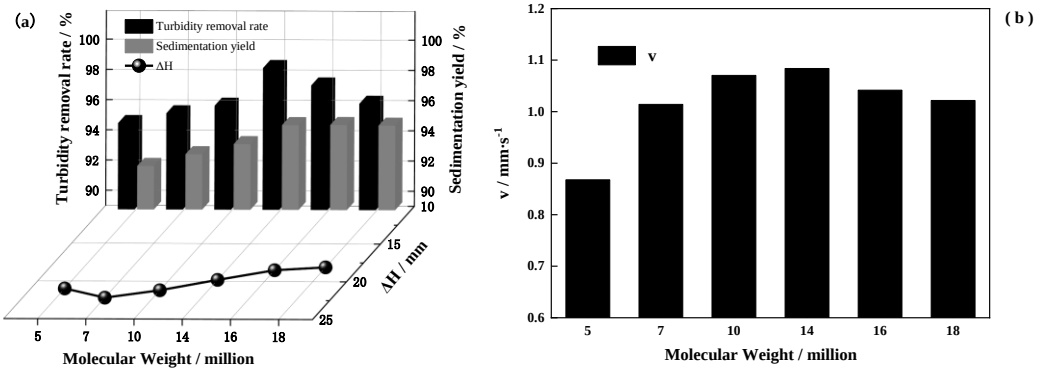

Fig. 3. Effect of molecular weight of NPAM on flocculation sedimentation experiment results

is because the NPAM is a linear polymer, when its low molecular weight, molecular chain is shorter, and the ability of the network capture and bridging is weak. The formation of floccules is smaller and the ability to capture fine particles is also poor, so consequently the turbidity removal rate and sedimentation yield are low. At the same time, the formed flocs are small and dispersed, resulting in a low compaction of sedimentation products. With the increase in molecular weight, its molecular chain is also increased, as is its polymer bridging ability. The formed flocs packed more closely, and the sedimentation products will increase and compact closely. So the height of the compressed body increases first and then decreases continuously.

As one of the important indices of flocculation sedimentation, the settling velocity determines the economic benefit of coal washery to a certain extent. In this paper the settling velocity of montmorillonite suspension with different molecular weight NPAM is measured, and the results are shown in Fig. 3 (b). As can be seen from Fig. 3 (b), with the continuous rise in the molecular weight of NPAM, the initial settling rate continues to accelerate, and when the molecular weight is over 14 million, the initial settling rate begins to slow down. This is because when the molecular weight is too high, the flocs formed are large and dispersed, and crowd but repel each other in the settling process. Thus slowing down the settling rate is convincingly confirmed with the above three experimental indices. Based on this, it can be concluded that the molecular weight of the best NPAM used for the montmorillonite sample is 14 million, which will be tested later.

3.1.2. Influence of NPAM dosage on flocculation sedimentation

According to the above experimental results, using a fixed NPAM molecular weight of 14 million, the effect of different dosages of NPAM on montmorillonite flocculation settlement test were studied. The results are shown in Fig. 4. As can be seen from the results of Fig.4 (a) and (b), the variation rules of turbidity removal rate, sedimentation yield, compression body height (ΔH) and initial settlement velocity are consistent, showing a trend of rapid increase at first, and then basically maintaining a stable trend. This is basically consistent with previous studies (Wang et al., 2020). This is because NPAM achieves the flocculation and sedimentation of montmorillonite through polymer bridging and net

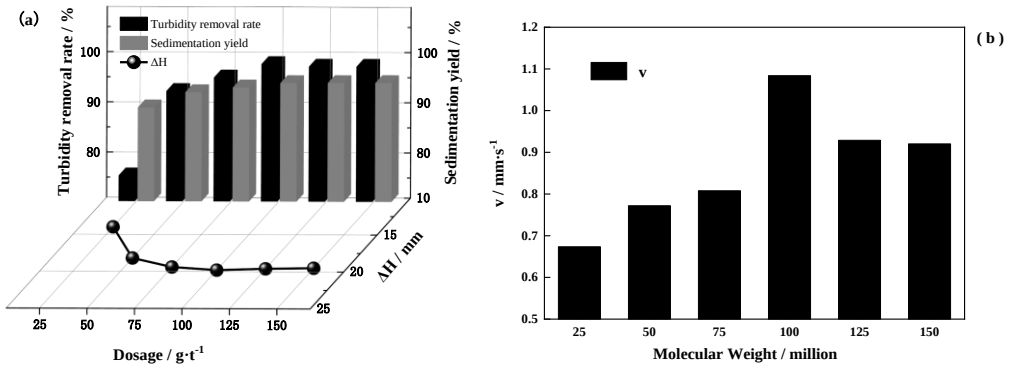

Fig. 4. Effect of NPAM dosage on flocculation and sedimentation experiment results

sweeping. In the montmorillonite suspension system, NPAM hydrolyzes to produce molecular chains, and these long molecular chains attract montmorillonite particles through Van Der Waals force. With the increase in dosage, a large number of long chains will be hydrolyzed, which will enhance the polymer bridging effect. At the same time, these extended long chains will crisscross each other in the suspension system, forming a network structure. With the dosage increasing the network structure will also increase, which will capture more suspended particles, thus accelerating the flocculation settlement effect. However, when the dosage of reagent is too much, the mineral surface is gradually completely covered, leaving fewer and fewer unoccupied adsorption sites for bridging flocculation. The tails and loops of linear polyacrylamide chains form and extend into an aqueous solution, and spatial stability occurs (Dash et al., 2011;Yan and Zhang, 2014) .These results mean that: the best dosage is 100g/t, the turbidity removal rate is 98.39%, the sedimentation rate is 94.62%, and the height of the compressed body is 19.80mm.

3.1.3. Analysis of Zeta potential results

The main purpose of Zeta potential measurement is to measure the change of the surface potential of montmorillonite before and after adding NPAM, so as to explain the mechanism of interaction between NPAM and montmorillonite particles. That is, the effect of the addition of NPAM on the degree of mutual exclusion or attraction of mineral particles. The Zeta potential test was conducted on montmorillonite particles and the montmorillonite particles after flocculation with NPAM 100g/t, and the test results are shown in the Fig. 5.

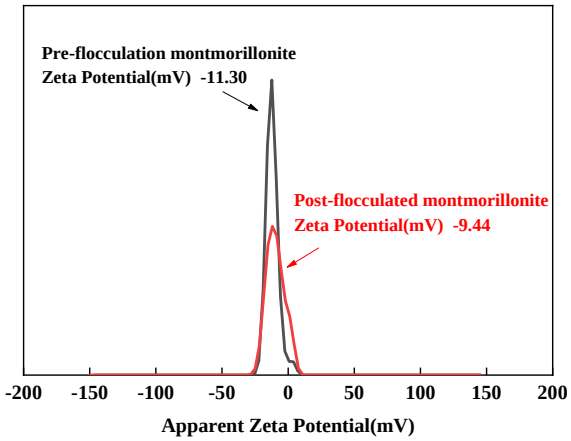

Fig. 5. Zeta potential of montmorillonite particles before and after NPAM addition

Fig. 5 shows that the montmorillonite particles have a charge of -11.19 mV on its surface, but after adding NPAM, its surface charge changes to -9.44 mV. Although the polymer NPAM is non-ionic, the surface charge of oxide plays an important role in the adsorption process. The adsorption of NPAM on montmorillonite can make the shear plane of the double electric layer of montmorillonite away from the surface, thus reducing the size of zeta potential. That is to say, with the increase of interaction between particles, flocs begin to form, thus losing stability and improving flocculation sedimentation effect (Sabah and Erkan, 2006; Dwari et al., 2018; Wang et al., 2020). The size and strength of flocs will be analysed and discussed as follow, and the microscopic charge transfer will be analysed in the simulation results.

3.1.4. Size analysis of floc size

The molecular weight of 14 million NPAM is configured to 0.05% solution, respectively, according to the dosage of 25g/t, 50g/t, 75g/t, 100g/t, 125g/t and 150g/t, added to the concentration of 20g/L montmorillonite suspension. After the settlement of montmorillonite suspension and the clarification of supernatant, the bottom floc was sucked out with a long rubber head dropper and dropped onto the glass slide. The glass slide was moved to the metallographic microscope for floc morphology observation. The results are shown in Fig. 6.

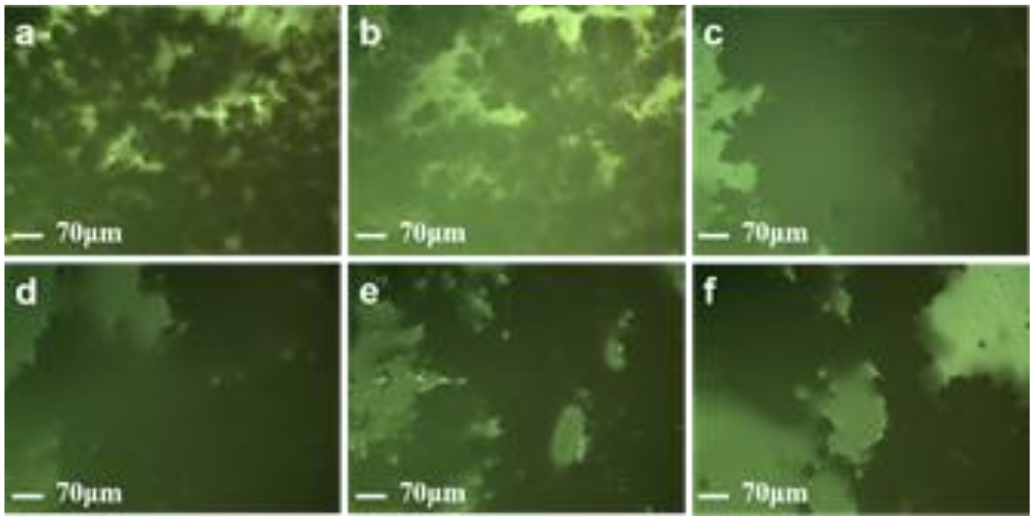

Fig. 6. The size of montmorillonite flocs was obtained using NPAM at 25g/t (a), 50g/t (b), 75g/t (c), 100g/t (d), 125g/t (e) and 150g/t (f) dosages, respectively

The flocculation effect is closely related to the physical properties of the floc itself. The size and strength of the floc have an impact on the flocculation effect. When the flocs are loose, the sedimentation rate is slow, so the sedimentation effect is relatively poor. In contrast, when the flocs are close the sedimentation rate is fast and the sedimentation effect is good. As can be seen from the results in Fig. 6, within a certain dosage range, with the increase of the dosage of the agent, the flocs also grow. When the dosage of the agent was 100g/t, the flocs formed were the largest and most compact ones, and the flocs diminished with the continuous increase of the dosage of agent. This was consistent with the experimental results of flocculation settlement. NPAM is a water-soluble polymer or polyelectrolyte, and the polar genes in its molecular chain can adsorb the suspended solid particles in water. A large electrostatic repulsion occurs between the particles when the dosage is small, and this repulsion plays a dominant role. Consequently, the particles are unable to get close to each other and it is difficult to form flocculent. When the dosage of NPAM increased, the adsorption and bridging effect of NPAM began to strengthen, so that larger flocs were formed between particles. This helped to achieve the accelerating settlement, and it had a very obvious flocculation and settlement effect.

3.1.5. Micromorphology analysis of flocs

SEM analysis was carried out on the montmorillonite suspension with the dosage of NPAM of 0g/t, 12.5g/t, 25g/t, 50g/t, 75g/t, 100g/t, 125g/t and 150g/t, respectively. Here the objective was to observe the surface morphology and structure of the flocs, and the NPAM molecular weight was 14 million. The results are shown in Fig. 7.

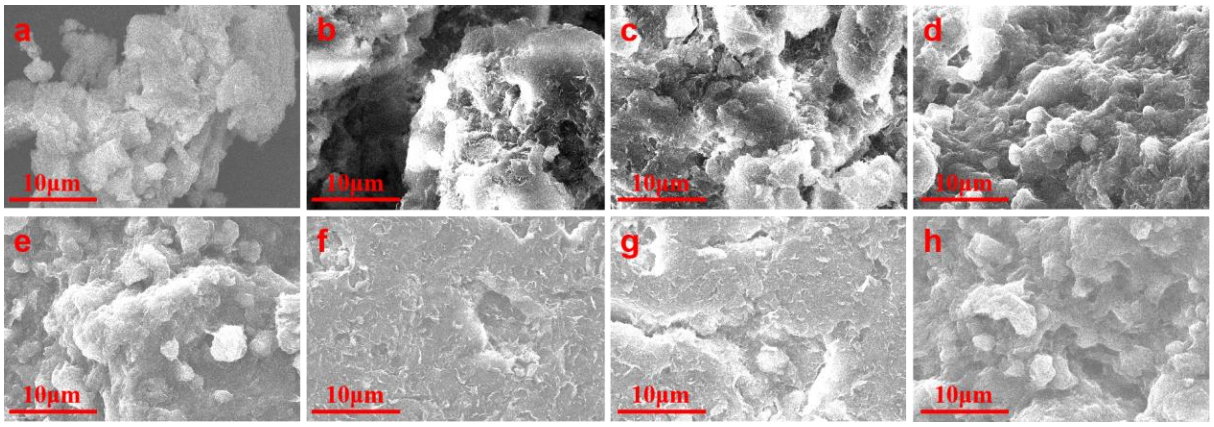

Fig.7. SEM image of montmorillonite flocs under the action of NPAM at 0g/t (a), 12.5g/t (b),25g/t (c), 50g/t (d), 75g/t (e), 100g/t (f), 125g/t (g) and 150g/t (h) dosages, respectively

When NPAM was added to the montmorillonite suspension, the mineral particles quickly formed flocs and dropped, and the supernatant was gradually clarified, obtaining the obvious flocculation settlement effect. Results can be seen from Fig. 7. When the flocculant dosage is less than 100g/t, with the increase of dosage, floccules start to increase and get closer to each other, forming a unique multi-level close three-dimensional network structure. The reason for this is that the PAM flocculant used in the experiment is a polymer compound, chaining with a number of active groups, which can adsorb suspended particles, and the polymer bridging action will gather solid particles together and produce precipitation. When the dosage of the flocculant is more than 100g/t, the compactness between the flocs decreases and pores begin to appear. This is because the surface of the colloidal particles formed by adsorption must retain enough space to bridge with another colloidal particle, otherwise the bridging cannot be successful. In other words, the flocculation settlement cannot be carried out. In particular, if the dosage of the agent is more than a lot, it will produce flocculation protection instead. Therefore, NPAM has an optimal dosage that can be used. Before reaching the best possible dosage, when the dosage increases the flocculation effect will continue to improve. At the optimal dosage, the flocculation effect is the best. If the dosage exceeds this value then the flocculation effect will diminish.

Flocculation sedimentation experiment can only reveal the flocculation behavior between NPAM with montmorillonite particles from a macro perspective. Molecular simulation technology is a powerful tool for analyzing the microscopic properties of substances. By selecting the classical theoretical methods and constructing a reasonable system, the mechanism of action between reagents and mineral surfaces can be studied from a microscopic point of view. The NPAM used in the flocculation sedimentation experiment is polymerized by AM monomer. For this reason the AM molecular was selected as the adsorbate in this paper to explore the micro-mechanism of NPAM and montmorillonite surface.

3.2. Density functional theory (DFT) analysis

3.2.1. Adsorption energies and configuration

In the process of geometric optimization of adsorption configuration, the AM molecule will move to a more reasonable position due to the interaction between the AM molecule and the surface atoms, and finally carries out stable adsorption at the position with the lowest adsorption energy. The adsorption energy can be used to indicate the stability of adsorption configuration: the lower adsorption energy is, the more stable adsorption configuration is. The calculation formula (4) of adsorption energy is written here (Peng et al., 2016):

$$E_{ads} = E_{total} - \left(E_{surface} + E_{adsorbate}\right) \tag{4}$$

In formula (4), Etotal represents the total energy of the system after the adsorption of AM molecules on the surface of montmorillonite crystal. Meanwhile Esurface and Eadsorbate respectively represent the surface energy of the montmorillonite crystal and the energy of the AM molecule before adsorption.

The adsorption configurations of AM molecules at different initial positions on montmorillonite surfaces of Na-(001) and None-(001) were geometrically optimized. According to the symmetry of the montmorillonite surface model, the initial adsorption sites of acrylamide on montmorillonite Na-(001) surface and None-(001) surface were constructed, and the results are illustrated in Fig. 8. In the figure, T, B, and H represent the Top sites, Bridge sites and Hollow sites, respectively. Then, the adsorption configurations of acrylamide at different initial positions of montmorillonite Na-(001) surface and None-(001) surface were geometrically optimized. The final adsorption positions and the adsorption energies of stable configurations are shown in Table 1.

According to the calculation results listed in Table 2, the adsorption energy of AM molecule on the Na-(001) surface ranges from -108.81 to -95.44 kJ/mol, and on the None-(001) surface ranges from -50.66 to -33.30 kJ/mol, indicating the existence of equilibrium cationic sodium ion. It can significantly enhance the adsorption stability of AM on the Na-(001) surface. According to the comparison of adsorption energies, the best adsorption sites of AM on the Na-(001) and None-(001) surfaces of montmorillonite were T3 and T1, respectively, and the corresponding adsorption energies were about -108.81 kJ/mol and -50.66 kJ/mol. At the same time, some research results show that PAM molecules can replace neatly ordered water molecules on the clay surface as a systematic spontaneous process (Yan and Zhang, 2014),

and the most stable adsorption energy of acrylamide molecules on the Na-(001) surface of montmorillonite calculated in this paper is about -108.265 kJ/mol, while the adsorption energy of water molecules on the (001) surface of montmorillonite is -62.4 kJ/mol (Peng et al., 2016), so it is easier for acrylamide molecules to replace the water molecules for adsorption on the surface of mineral particles. The bonding properties of these two adsorption configurations were analyzed. The two adsorption configurations are exhibited in Fig. 9., and the bonding information between the corresponding interacting atoms is listed in Table 3.

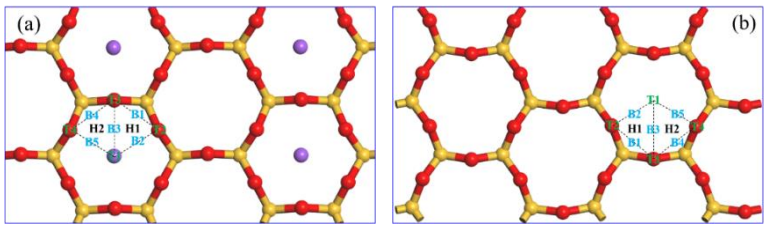

Fig. 8. The initial adsorption position of acrylamide on montmorillonite surface (a is Na-(001) surface, b is None-(001) surface)

Table 2. Adsorption energy of AM molecule adsorbed on Na-(001) and None-(001) surfaces of montmorillonite

Before	Na-(001)		None-(001)	
	After	Eads (kJ/mol)	After	Eads (kJ/mol)
T1	B1	-107.62	T1	-46.19
T2	T2	-104.62	T2	-33.97
T3	T3	-105.33	T3	-35.34
T4	T4	-99.10	T4	-36.12
B1	T3	-105.33	T2	-38.38
B2	B1	-99.10	T2	-40.99
B3	T3	-108.81	T4	-41.81
B4	T3	-99.03	B4	-33.30
B5	T4	-95.44	B5	-44.55
H1	T3	-101.10	T1	-49.44
H2	T3	-99.93	T1	-50.66

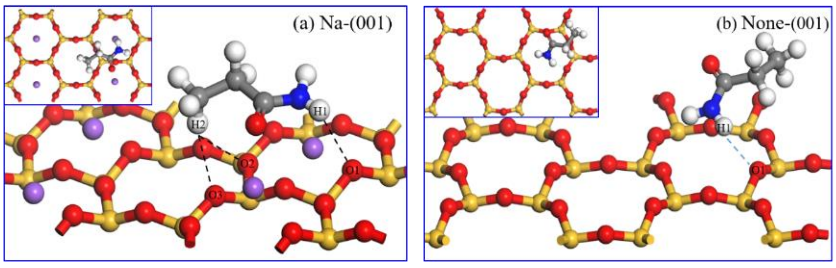

Fig. 9. The best adsorption configurations of AM molecules on Na-(001) and None-(001) surfaces of montmorillonite

Table 3. The bonding information between AM and montmorillonite surface

Model	Bond	d(X-H…O)/Å	D(X-H…O)/Å	θ(H-X…O)/°
Na-(001)	H1--O1	2.607	3.224	45.340
	H2--O2	2.680	3.540	32.433
	H2--O3	2.778	2.778	39.698
None-(001)	H1…O1	2.410	3.266	27.649

(Annotation: … means hydrogen bonds exist between atoms, -- means no hydrogen bonds exist between atoms)

According to the theory of (Luzar and Chandler, 1993), combined with the data in the Table 3, it can be seen that AM molecule does not form hydrogen bonds with the Na-(001) surface of montmorillonite, but with the None-(001) surface. In the Fig. 9, the blue dotted line indicates the hydrogen bond effect, while the black dotted line indicates the non-hydrogen bond interaction between the connected atoms. However, the adsorption energy of the AM molecule on the Na-(001) surface is significantly lower than that on the None-(001) surface. Indicated here is that there is a non-hydrogen bond on the Na-(001) surface, which is greater than the weak hydrogen bond formed on the None-(001) surface. Studies have shown that the basic oxygen on the siloxane surface of layered silicate minerals is a very weak electron donor and cannot form hydrogen bonds with non-ionic polymers (Deng et al., 2006). This is consistent with the conclusion of this paper.

3.2.2. Partial density of states analysis

In order to better analyze the bonding, orbital and atomic activity of the main interacting atoms between the adsorbent and the surface, H1--O1 formed by AM molecule on Na-(001) surface of montmorillonite and H1…O1 formed by None-(001) surface were selected to analyze the changes of density of states of the corresponding interacting atoms before and after adsorption. The results are shown in Fig. 10.

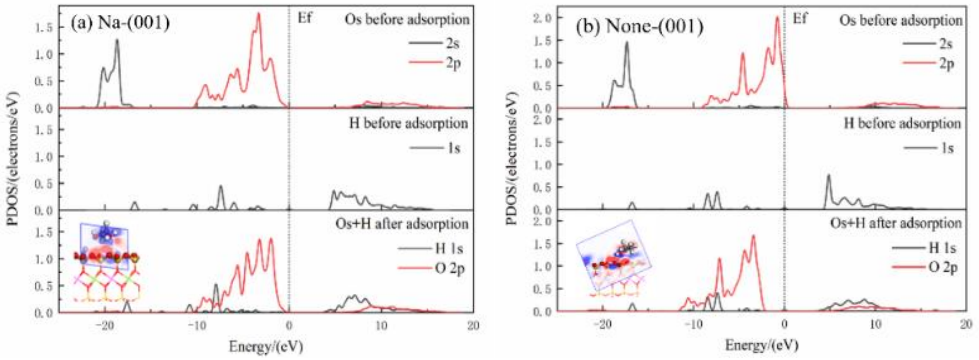

Fig. 10. Density of states of AM molecules before and after adsorption on Na-(001) and None-(001) surfaces of montmorillonite

According to the density of states analysis, after the adsorbent AM molecule is adsorbed on the surface, the electron density of states near the Fermi level decreases, and the energy of O2p moves from the former one to the lower level, strongly suggesting that the surface energy decreases after adsorption. According to Fig. 10, when the AM molecule is adsorbed on the surface of montmorillonite Na-(001), the 1s orbital of the hydrogen atom H1 in the molecule does not bond with the 2p orbital of the oxygen atom O1 on the surface. When the AM molecule is adsorbed on the surface of montmorillonite None-(001), the 1s orbital of the hydrogen atom H1 and the 2p orbital of the oxygen atom O1 have a bonding effect between -11.5 eV and -2.0eV. Meanwhile there is an antibonding effect between 3.5 eV and 15.0eV. The bonding effect is stronger than the antibonding. Combined with the adsorption energy, it is further indicated that there is a non-hydrogen bonding effect on the adsorption of AM molecules on the surface of montmorillonite Na-(001), which is greater than the weak hydrogen bond effect formed on the surface of None-(001). This outcome confirms that the hydrogen bonding effect is not the main reason for the adsorption of AM molecules on the montmorillonite surface.

3.2.3. Charge and electron density difference analysis

Electron density difference can visually represent the charge transfer between bonding atoms or adjacent atoms when the adsorbent AM molecule is adsorbed on the surface of montmorillonite. The electron density difference map of AM molecule adsorbed on Na-(001) and None-(001) surfaces of montmorillonite is shown in Fig. 11. The blue area indicates increased electron density and the yellow area indicates decreased electron density. At the same time, Table 4 lists the Mulliken charge populations of hydrogen atoms in AM molecules and oxygen atoms on the surface of montmorillonite

directly interacting with them before and after adsorption. In the meantime, the charge changes of AM molecules and montmorillonite surface models before and after adsorption are calculated.

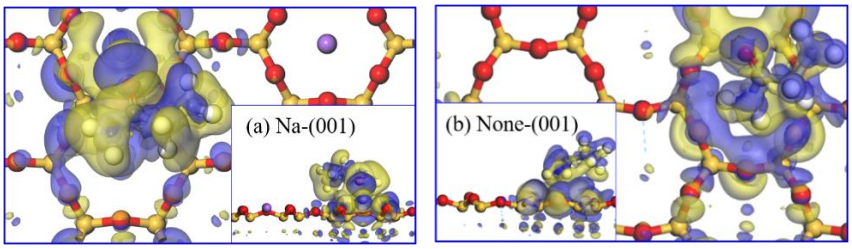

Fig. 11. The electron density difference of the optimal adsorption configurations of AM molecules on the Na-(001) and None-(001) surfaces of montmorillonite

Table 4. Mulliken population/charge analysis and surface charge analysis of AM molecules before and after adsorption on Na-(001) and None-(001) surfaces of montmorillonite

Model	Name	Before				After			
		s	p	Total	charge/e	s	p	Total	charge/e
Na-(001)	H1	0.53	0	0.53	0.47	0.62	0	0.62	0.38
	H2	0.71	0	0.71	0.29	0.74	0	0.74	0.26
	O1	1.84	5.3	7.14	-1.14	1.84	5.3	7.15	-1.15
	O2	1.84	5.31	7.15	-1.15	1.84	5.31	7.15	-1.15
	O3	1.84	5.31	7.15	-1.15	1.84	5.32	7.15	-1.15
	AM				0				-0.21
	Na-(001)				0				0.21
None-(001)	H1	0.55	0	0.55	0.45	0.58	0	0.58	0.42
	O1	1.84	5.31	7.15	-1.15	1.84	5.31	7.15	-1.15
	AM				0				-0.05
	None-(001)				0				0.05

From Fig. 11, there is a significant charge transfer between the bonding atoms or adjacent atoms between AM molecules and Na-(001) and None-(001) surfaces of montmorillonite. This can be observed from Figure 10 (b), regarding the adsorption system between AM molecules and montmorillonite None-(001) surfaces. In addition to the charge transfer between H1 and O1, which directly form hydrogen bonds, other atoms in the adsorbent also enrich and consume electron density between atoms close to the surface, meaning that there is no direct relationship between the formation of hydrogen bonds and charge transfer. The data in Table 4 show that (0.03 ~ 0.09) e is obtained from the 1s state of hydrogen atom interacting with oxygen atom on the surface of Na-(001), and 0.03e is obtained from the 1s state of hydrogen atom interacting with oxygen atom on the surface of None-(001). However, the Mulliken charge population of oxygen atoms on the surface of montmorillonite changed little after adsorption of the AM molecule. The transfer charge of the AM molecule on the surface of montmorillonite Na-(001) was 0.21e, which was significantly greater than that on the None-(001) surface of montmorillonite with 0.05e. The more transfer charge there was between the adsorbent and the surface, the smaller the adsorption energy was, and the more stable the adsorption system remained. This finding is consistent with the calculation results of adsorption energy. This is consistent with the conclusion that NPAM reduces the surface negative charge of montmorillonite particles by Zeta potential test. Combining the results of electron density difference and Mulliken charge population analysis, the following summation can be made. Although no hydrogen bond was formed on the Na-(001) surface of montmorillonite, the transfer charge of the AM molecule was significantly greater than that on None-(001) surface, resulting in the adsorption between the AM molecule and the Na-(001) surface. What made this possible was electrostatic attraction, and the electrostatic attraction was stronger than the hydrogen bond, occupying the dominant position.

The results of flocculation sedimentation experiment showed that the addition of NPAM could improve the sedimentation effect of montmorillonite suspension, which was consistent with the results of molecular simulation that AM molecules had an adsorption effect on the surface of montmorillonite. With the increase of molecular weight, the molecular chain of NPAM will also increase, and more active groups will combine with more adsorption sites on the surface of montmorillonite, especially on the Na- (001) surface. This process will produce stronger adsorption and improve the flocculation and sedimentation effect. At the same time, the increase in the dosage of the reagent will hydrolyze a large number of long chains and increase the contact opportunities with the surface. The adsorption effect caused by the electrostatic attraction is stronger and the flocculation sedimentation effect is significantly increased. However, when the dosage of the reagent is too large, the adsorption effect has reached saturation and the flocculation effect will not increase significantly. The molecular simulation results more intuitively verified the action behavior of NPAM with montmorillonite particles from a microscopic perspective, and revealed the action mechanism between them.

4. Conclusions

In this paper, the flocculation behavior and law between NPAM and ultrafine montmorillonite particles were studied through flocculation sedimentation test. The flocculation mechanism between NPAM and ultrafine montmorillonite particles was revealed by microscopic floc morphology observation and density functional theory calculation. The main conclusions are as follows :

1) As the molecular weight of NPAM increases, the flocculation sedimentation effect is constantly improved. When the molecular weight of NPAM is too large, the adsorption effect has reached saturation, and the flocculation effect will not be significantly improved.

2) With the increase of the dosage of NPAM, the flocculation sedimentation effect is significantly improved. When the dosage of NPAM is too large, the surface of the colloidal particles formed by adsorption does not have enough space to bridge with another long chain of colloidal particles, and the sedimentation effect decreases.

3) The observation results of floc morphology demonstrated that the floc size increased was the NPAM dosage increased. The reason was that a number of active groups on the NPAM chain could aggregate solid particles together through polymer bridging to generate precipitation, forming a unique multi-level compact spatial three-dimensional network structure.

4) DFT calculation results showed that acrylamide molecule did not form hydrogen bonds with montmorillonite Na-(001) surface, and its adsorption energy was -108.81 kJ/mol. This was significantly higher than that of -50.66 kJ/mol, which formed a hydrogen bond on None-(001) surface. Based on the analysis results of adsorption energy, density of states and electron density difference, it can be concluded that: hydrogen bonding is not the main reason for the adsorption of acrylamide on the montmorillonite surface, while electrostatic attraction plays a leading role.

Acknowledgments

The financial supports for this work from the National Natural Science Foundation of China under the grant No. 51874011, the National Natural Science Foundation of China under the grant No. 51804009, and the Key Research and Development Plan Projects in Anhui Province (202004a07020044) are gratefully acknowledged.

References

AKIMKHAN, A.M., 2013. *Adsorption of polyacrylic acid and polyacrylamide on montmorillonite.* Russ. J. Phys. Chem. A 87, 1875–1880.

BAI, H., LIU, Y., ZHAO, Y., CHEN, T., CHEN, L., JIAO, X., QING, C., SONG, S., 2020. *Effects of clay species on coal flotation under the cationic regulation.* Chem. Phys. Lett. 753, 137626.

CHEN, J., MIN, F., LIU, L., 2019. *The interactions between fine particles of coal and kaolinite in aqueous, insights from experiments and molecular simulations.* Appl. Surf. Sci. 467–468, 12–21.

CHEN, J., Min, F., PENG, C., LIU, C., CHEN, S., CHEN, C., 2015. *Characteristics of the hydrophobic aggregation of fine particles in coal slurry water under the action of quaternary ammonium salt.* Zhongguo Kuangye Daxue Xuebao/Journal China Univ. Min. Technol. 44, 332–340.

DASH, M., DWARI, R.K., BISWAL, S.K., REDDY, P.S.R., CHATTOPADHYAY, P., MISHRA, B.K., 2011. *Studies on the effect of flocculant adsorption on the dewatering of iron ore tailings.* Chem. Eng. J. 173, 318–325.

DENG, Y., DIXON, J.B., WHITE, G.N., LOEPPERT, R.H., JUO, A.S.R., 2006. *Bonding between polyacrylamide and smectite.* Colloids Surfaces A Physicochem. Eng. Asp. 281, 82–91.

DOI, A., EJTEMAEI, M., NGUYEN, A. V., 2019. *Effects of ion specificity on the surface electrical properties of kaolinite and montmorillonite.* Miner. Eng. 143, 105929.

DWARI, R.K., ANGADI, S.I., TRIPATHY, S.K., 2018. *Studies on flocculation characteristics of chromite's ore process tailing: Effect of flocculants ionicity and molecular mass.* Colloids Surfaces A Physicochem. Eng. Asp. 537, 467–477.

FENG, L., TANG, H.Y., LIU, J.T., SONG, L.L., 2013. *Adsorption thermodynamics, kinetics and mechanism of calcium(II) ions onto kaolinite clay in coal slime water.* Asian J. Chem. 25, 3927–3930.

FIJALKOWSKA, G., WIŚNIEWSKA, M., SZEWCZUK-KARPISZ, K., 2019. *Studies of the Cationic Polyacrylamide Adsorption on the Montmorillonite Surface in the Presence of Lead(II) Ions.* Proceedings 16, 28.

FORRER, D., VITTADINI, A., 2019. *A DFT-D2 study of formic acid adsorption at smectite edges based on pyrophyllite models.* Chem. Phys. Lett. 733, 136687.

GONG, G., ZHANG, Y., ZHENG, H., LIU, G., LI, Y., SHI, K., 2016. *Experimental study on the transmittance of the supernatant of refractory slime water.* J. Chem. Eng. Japan 49, 417–424.

GUO, W., ZHANG, H., MA, Z., 2019. *Study of Synthesis and Flocculation Properties of New Modified Hydrophobic Organic Polymer P(AM-DM-DMC12).* Int. J. Polym. Sci. 2019.

HAN, Y., LIU, W., CHEN, J., 2016. *DFT simulation of the adsorption of sodium silicate species on kaolinite surfaces.* Appl. Surf. Sci. 370, 403–409.

KIM, Y., KIM, C., KIM, J., KIM, Y., LEE, J., 2020. *Experimental investigation on the complex chemical reactions between clay minerals and brine in low salinity water-flooding.* J. Ind. Eng. Chem. 89, 316–333.

LI, Q., SHI, W., YANG, Q., 2021. *Polarization induced covalent bonding: A new force of heavy metal adsorption on charged particle surface.* J. Hazard. Mater. 412, 125168.

LI, Y., XIA, W., WEN, B., XIE, G., 2019. *Filtration and dewatering of the mixture of quartz and kaolinite in different proportions.* J. Colloid Interface Sci. 555, 731–739.

LIN, Z., YANG, C., SHEN, Z., QI, X., 2010. *The properties and sedimentation characteristics of extremely sliming coal slime water.* Meitan Xuebao/Journal China Coal Soc. 35, 312–315.

LOU, Z., LIU, H., ZHANG, Y., MENG, Y., ZENG, Q., SHI, J., YANG, M., 2014. *A density functional theory study of the hydration of calcium ions confined in the interlayer space of montmorillonites.* J. Theor. Comput. Chem. 13, 1–13.

LUZAR, A., CHANDLER, D., 1993. *Structure and hydrogen bond dynamics of water-dimethyl sulfoxide mixtures by computer simulations.* J. Chem. Phys. 98, 8160–8173.

MA, X., FAN, Y., DONG, X., CHEN, R., LI, H., SUN, D., YAO, S., 2018. *Impact of clay minerals on the dewatering of coal slurry: An experimental and molecular-simulation study.* Minerals 8.

MCFARLANE, A., YEAP, K.Y., BREMMELL, K., ADDAI-MENSAH, J., 2008. *The influence of flocculant adsorption kinetics on the dewaterability of kaolinite and smectite clay mineral dispersions.* Colloids Surfaces A Physicochem. Eng. Asp. 317, 39–48.

MPOFU, P., ADDAI-MENSAH, J., RALSTON, J., 2004. *Flocculation and dewatering behaviour of smectite dispersions: Effect of polymer structure type.* Miner. Eng. 17, 411–423.

PENG, C., MIN, F., LIU, L., CHEN, J., 2016. *A periodic DFT study of adsorption of water on sodium-montmorillonite (001) basal and (010) edge surface.* Appl. Surf. Sci. 387, 308–316.

REN, B., MIN, F., CHEN, J., FANG, F., LIU, C., 2020. *Adsorption mechanism insights into CPAM structural units on kaolinite surfaces: A DFT simulation.* Appl. Clay Sci. 197, 105719.

SABAH, E., ERKAN, Z.E., 2006. *Interaction mechanism of flocculants with coal waste slurry*. Fuel 85, 350–359.

SHI, J., LIU, H., MENG, Y., LOU, Z., ZENG, Q., YANG, M., 2013. *First-principles study of ammonium ions and their hydration in montmorillonites.* J. Mol. Model. 19, 1875–1881.

SHI, J., LOU, Z., YANG, M., ZHANG, Y., LIU, H., MENG, Y., 2014. *Theoretical characterization of formamide on the inner surface of montmorillonite.* Surf. Sci. 624, 37–43.

SUN, X., LIU, W., YANG, Z., ZHUO, Q., ZHANG, H., GENG, P., 2021. *DFT study of the adsorption of 2,3-epoxypropyltrimethylammonium chloride on montmorillonite surfaces.* J. Mol. Liq. 334, 116145.

VANEREK, A., ALINCE, B., VAN DE VEN, T.G.M., 2006. *Delamination and flocculation efficiency of sodium-activated kaolin and montmorillonite. Colloids Surfaces A Physicochem.* Eng. Asp. 273, 193–201.

VOORA, V.K., AL-SAIDI, W.A., JORDAN, K.D., 2011. *Density functional theory study of pyrophyllite and M-montmorillonites (M = Li, Na, K, Mg, and Ca): Role of dispersion interactions.* J. Phys. Chem. A 115, 9695–9703.

WANG, B., XU, W., FU, J., WANG, W., XIAO, X., 2019. *Preparation of two nanometer magnetic flocculants and treatment of slime wastewater.* IOP Conf. Ser. Earth Environ. Sci. 345.

WANG, C., SUN, C., LIU, Q., 2020. *Formation, breakage, and re-growth of quartz flocs generated by non-ionic high molecular weight polyacrylamide.* Miner. Eng. 157, 106546.

WANG, S., SONG, X., WANG, X., CHEN, Q., QIN, J., KE, Y., 2020. *Influence of coarse tailings on flocculation settlement.* Int. J. Miner. Metall. Mater. 27, 1065–1074.

WIŚNIEWSKA, M., FIJALKOWSKA, G., SZEWCZUK-KARPISZ, K., 2018. *The mechanism of anionic polyacrylamide adsorption on the montmorillonite surface in the presence of Cr(VI) ions.* Chemosphere 211, 524–534.

WIŚNIEWSKA, M., FIJALKOWSKA, G., SZEWCZUK-KARPISZ, K., URBAN, T., NOSAL-WIERCIŃSKA, A., WÓJCIK, G., 2019. *Comparison of adsorption affinity of anionic and cationic polyacrylamides for montmorillonite surface in the presence of chromium(VI) ions.* Adsorption 25, 41–50.

YAN, X., WEI, L., MENG, Q., WANG, J., YANG, Q., ZHAI, S., LU, J., 2021. *A study on the mechanism of calcium ion in promoting the sedimentation of illite particles.* J. Water Process Eng. 42, 102153.

YAN, X., ZHANG, X., 2014. *Interactive effects of clay and polyacrylamide properties on flocculation of pure and subsoil clays.* Soil Res. 52, 727–737.

YANG, Z., LIU, W., ZHANG, H., JIANG, X., MIN, F., 2018. *DFT study of the adsorption of 3-chloro-2-hydroxypropyl trimethylammonium chloride on montmorillonite surfaces in solution.* Appl. Surf. Sci. 436, 58–65.

YU, Y., MA, L., CAO, M., LIU, Q., 2017. *Slime coatings in froth flotation: A review.* Miner. Eng. 114, 26–36.

ZHAO, Y., MENG, L., SHEN, X., 2020. *Study on ultrasonic-electrochemical treatment for difficult-to-settle slime water.* Ultrason. Sonochem. 64, 104978.

ZHU, S., KHAN, M.A., WANG, F., BANO, Z., XIA, M., 2021. *Exploration of adsorption mechanism of 2-phosphonobutane-1,2,4-tricarboxylic acid onto kaolinite and montmorillonite via batch experiment and theoretical studies.* J. Hazard. Mater. 403, 123810.